AFRL-RX-WP-TP-2011-4207

MICROSTRUCTURE INSTABILITY IN CRYOGENICALLY-DEFORMED COPPER (PREPRINT)

S.L. Semiatin

Metals, Ceramics, and NDE Division

T. Konkova, S. Mironov, and A. Korznikov

Russian Academy of Science

MARCH 2011

AIR FORCE RESEARCH LABORATORY
MATERIALS AND MANUFACTURING DIRECTORATE
WRIGHT-PATTERSON AIR FORCE BASE, OH 45433-7750
AIR FORCE MATERIEL COMMAND
UNITED STATES AIR FORCE

REPORT DOCUMENTATION PAGE

Form Approved
OMB No. 0704-0188

1. REPORT DATE *(DD-MM-YY)*	2. REPORT TYPE	3. DATES COVERED *(From - To)*
March 2011	Journal Article Preprint	01 March 2011 – 01 March 2011

4. TITLE AND SUBTITLE
MICROSTRUCTURE INSTABILITY IN CRYOGENICALLY-DEFORMED COPPER (PREPRINT)

5a. CONTRACT NUMBER
In-house

5b. GRANT NUMBER

5c. PROGRAM ELEMENT NUMBER
62102F

6. AUTHOR(S)
S.L. Semiatin (AFRL/RX)
T. Konkova, S. Mironov, and A. Korznikov (Russian Academy of Science)

5d. PROJECT NUMBER
4347

5e. TASK NUMBER
20

5f. WORK UNIT NUMBER
25100102

7. PERFORMING ORGANIZATION NAME(S) AND ADDRESS(ES)

Metals, Ceramics, and NDE Division (AFRL/RX)
Air Force Research Laboratory
Materials and Manufacturing Directorate
Wright-Patterson Air Force Base, OH 45433-7750
Air Force Materiel Command
United States Air Force

Russian Academy of Science
Institute for Metals Superplasticity Problems
39 Khalturin Street
Ufa, 450001, Russia

8. PERFORMING ORGANIZATION REPORT NUMBER
AFRL-RX-WP-TP-2011-4207

9. SPONSORING/MONITORING AGENCY NAME(S) AND ADDRESS(ES)
Air Force Research Laboratory
Materials and Manufacturing Directorate
Wright-Patterson Air Force Base, OH 45433-7750
Air Force Materiel Command
United States Air Force

10. SPONSORING/MONITORING AGENCY ACRONYM(S)
AFRL/RXLM

11. SPONSORING/MONITORING AGENCY REPORT NUMBER(S)
AFRL-RX-WP-TP-2011-4207

12. DISTRIBUTION/AVAILABILITY STATEMENT
Approved for public release; distribution unlimited.

13. SUPPLEMENTARY NOTES
PAO Case Number: 88ABW 2010-2660; Clearance Date: 15 May 2010. Document contains color.
Journal article submitted to *Scripta Materialia.*

14. ABSTRACT
There is considerable interest in the potential use of cryogenic deformation for the production of nanocrystalline materials. It is believed that low homologous temperatures may suppress dynamic recovery and stimulate mechanical twinning, thus enhancing the refinement of grain size. The subsequent ambient-temperature stability of the microstructures thus produced is an important consideration with regard to practical use of such processing approaches. For example, primary recrystallization during static storage at room temperature has been observed in cryogenically-rolled copper. This unusual phenomenon was hypothesized to be associated with a high density of vacancies in the cryo-deformed material giving rise to the exceptionally high grain-boundary mobility. It may also be conjectured that such instabilities may be exacerbated with an increase in the imposed cryogenic strain such as is common during severe plastic deformation. The objective of the present work was to quantify in more detail such microstructural instability.

15. SUBJECT TERMS
cryogenic deformation; electron backscattering diffraction; copper; nanocrystalline microstructure; abnormal grain growth

16. SECURITY CLASSIFICATION OF:			17. LIMITATION OF ABSTRACT:	18. NUMBER OF PAGES	19a. NAME OF RESPONSIBLE PERSON (Monitor)
a. REPORT	b. ABSTRACT	c. THIS PAGE			Donna L. Ballard
Unclassified	Unclassified	Unclassified	SAR	16	19b. TELEPHONE NUMBER *(Include Area Code)* N/A

Microstructure instability in cryogenically-deformed copper

T. Konkova[1], S. Mironov[1,2], A. Korznikov[1], and S.L. Semiatin[3]

[1]Institute for Metals Superplasticity Problems, Russian Academy of Science, 39 Khalturin Str., Ufa, 450001, Russia
[2]Department of Materials Processing, Graduate School of Engineering, Tohoku University, 6-6-02 Aramaki-aza-Aoba, Sendai 980-8579, Japan
[3]Air Force Research Laboratory, Materials and Manufacturing Directorate, AFRL/RXLM, Wright-Patterson AFB, OH 45433-7817, USA

High-resolution electron backscatter diffraction (EBSD) was employed to establish the stability of microstructure in severely cryo-deformed copper during long-term static storage at room temperature. The material was shown to exhibit grain growth including some aspects of abnormal grain growth.

Keywords: Cryogenic deformation; Electron backscattering diffraction; Copper; Nanocrystalline microstructure; Abnormal grain growth

There is considerable interest in the potential use of cryogenic deformation for the production of nanocrystalline materials [e.g. 1-3]. It is believed that low homologous temperatures may suppress dynamic recovery and stimulate mechanical twinning [2,3] thus enhancing the refinement of grain size. The subsequent ambient-temperature stability of the microstructures thus produced is an important consideration with regard to practical use of such processing approaches. For example, primary recrystallization during static storage at room temperature has been observed in cryogenically-rolled copper [4,5]. This unusual phenomenon was hypothesized to be associated with a high density of vacancies in the cryo-deformed material giving rise to the exceptionally high grain-boundary mobility [4]. It may also be conjectured that such instabilities may be exacerbated with an increase in the imposed cryogenic strain such as is common during severe plastic deformation. The objective of the present work was to quantify in more detail such microstructural instability. For this purpose, microstructure changes occurring in severely cryo-deformed copper during long-term storage at room temperature were documented.

The program material consisted of commercial-purity copper whose nominal chemical composition is given in Table 1. The as-received hot-rolled bar was preconditioned by severe "abc" deformation in the temperature range of 500-300°C [6]. Following forging, disk-shaped samples measuring 10 mm in diameter and 2 mm in thickness were cut from the central part of the billet and subjected to cryogenic deformation via high pressure torsion (HPT) under an applied pressure of 4.5 GPa. The imposed deformation comprised 20 consecutive, fully-reversed 45° rotations in the clockwise and counter-clockwise directions. To provide cryogenic-deformation conditions, each test sample and the tooling anvils were soaked in liquid nitrogen and held for 20 minutes prior to testing. Heat-transfer calculations revealed that the *warming* of the sample and anvils prior to HPT due to free convection in air was relatively small, resulting in temperature increases of

approximately 6°C and 3°C, respectively. Immediately after deformation, each sample was quenched in liquid nitrogen and kept at 77°K for approximately 1 year prior to examination.

Microstructure changes during static storage at room temperature were quantified for periods ranging from 2 weeks to 11 months. To provide a clear idea of microstructure evolution, all observations were made at nearly the same (mid-radius) location in a given sample. Microstructures were determined primarily via electron backscattering diffraction (EBSD). For this purpose, samples were prepared using conventional metallographic techniques followed by electropolishing in a solution of 70 pct. orthophosphoric acid in water at ambient temperature with an applied potential of 5 V. High-resolution EBSD analysis was conducted with a Hitachi S-4300SE field-emission-gun scanning electron microscope (FEG-SEM) equipped with a TSL OIM^{TM} EBSD system. All of the EBSD data were measured on the disk (shear) plane; the sample radial direction (RD) is vertical and the shear direction (SD) is horizontal in all results reported below. Specifically, EBSD scans consisted of ~400,000-500,000 pixels and were acquired with a step size of 25-100 nm. Although the spatial resolution of EBSD is a matter of ongoing debate, it is believed that its magnitude may be as low as ~10 nm in relatively high Z-number metals [7]; thus, a scan step size as small as 25 nm was reasonable. To minimize measurement errors, all grains comprising less than 3 pixels were automatically removed from the maps. Furthermore, to eliminate spurious boundaries caused by orientation noise, a lower limit boundary-misorientation cutoff of 2° was used. All misorientation angles quoted are relative to the rotation axis with the minimum misorientation. A 15° criterion was employed to define low-angle boundaries (LABs) versus high-angle boundaries (HABs).

All measurements of grain size were made by the linear-intercept method. Because the microstructures developed by SPD are frequently characterized by a complex mixture of HABs and LABs, there is often some confusion in the definition of grains. To clarify this issue, the term "grain" in the present work refers to a crystallite bordered by a continuous boundary having a misorientation of greater than 15°.

To obtain a broader view of underlying microstructure changes, the Vickers microhardness was also measured on each sample using a load of 50 g for 10 s. The effect of the static storage at room temperature on the microhardness profile across the sample diameter is shown in Fig. 1. After 15 minutes, the microhardness distribution was inhomogeneous; the well-known softening near the centre of the sample was found. After 11 months at room temperature, the distribution was much more uniform and, more importantly, the magnitude of microhardness was substantially lower. These measurements thus provided indirect evidence that the cryo-deformed material had experienced significant changes over time at ambient temperature.

EBSD microstructure maps of the cryo-deformed copper obtained after 2 weeks and 11 months at room temperature are shown in Fig. 2. The observations revealed major differences in grain structure. These differences were noticeable in maps taken with both the coarser step size of 100 nm (Fig. 2a,

c) and the finer step size of 25 nm (Fig. 2b, d). In all maps, LABs are depicted as red lines[1] and HABs as black lines.

The microstructure after 2 weeks at room temperature was reasonably homogeneous. It was dominated by nearly-equiaxed fine grains with an average size of ~0.3 μm (Fig. 2a). The grains contained a high density of LABs with various degrees of misorientation (Fig. 2b); the total LAB fraction constituted ~40% of total boundary area. Furthermore, it was found that a number of the high-angle grain boundaries were not straight but rather exhibited bulges that appeared to serve as the precursor to the formation of small grains; an example of this observation is circled in Fig. 2b. There were also isolated, relatively coarse grains in the microstructure (indicated by the arrow in Fig. 1a). These grains typically contained a very low orientation spread with almost no LABs; in other words, they appeared to be recrystallized.

After 11 months at room temperature, the microstructure was noticeably different (Fig. 2c). The principal feature of the microstructure after this longer time was the appearance of a number of abnormal, coarse (~10 μm) grains within a matrix of fine grains (~ 0.4 μm); i.e., the microstructure had become essentially bimodal (Fig. 2c). The very large difference between the grain sizes suggests that the material had undergone abnormal grain growth. The coarse, abnormal grains were typically free of LABs, but contained some coarse rectangular-shaped twins and even sporadic, fine, unconsumed equiaxed grains (Fig. 2c). Based on these observations, it may be concluded that the abnormal grains originated from the moderate-size, recrystallized grains found after 2 weeks at room temperature (indicated by the arrow in Fig. 2a). Because the number per unit volume and the size of the coarse grains were larger after 11 months (Fig. 2a vs 2c), it may also be concluded that the 2-week and 11-month observations represented different stages of the same abnormal grain-growth phenomenon. A comparison of the grain sizes in the *fine-grain regions* of the two samples (Fig. 2b vs 2d, Fig. 3a) suggested that these grains also underwent growth, albeit more normal-like, between 2 weeks and 11 months at room temperature.

The EBSD data were also used to quantify the evolution of the misorientation-angle distribution (Fig. 3b). These measurements were expressed in terms of specific grain-boundary length; i.e, the total grain-boundary length for a given misorientation angle (or small range of misorientation angles) divided by the area of the EBSD map. As shown below, this metric provides a better comparison of grain-boundary characteristics, thus enabling the key physical mechanisms governing microstructure evolution to be deduced reliably.

The EBSD measurements revealed that the specific length of grain boundaries in the misorientation-angle range of ~2-55° decreased with time in air. The reduction of HAB area is a consequence of grain growth discussed in the previous section. The migrating grain boundaries would also have eliminated some portion of the LABs, thus explaining the observed decrease in the specific length of such boundaries. Grain growth in some FCC metals (including copper) is known to be frequently accompanied by the formation of *annealing* twins [e.g.

[1] The reader is referred to on-line version of the paper to see the figures in color.

8]. Thus, the development of a sharp peak near 60° after 11 months is not surprising as well.

The operation of *mechanical* twinning has recently been reported in cryo-deformed copper [2,3]. In this regard, it is interesting to compare the fractions of mechanical and annealing twins in the microstructure. It is well accepted that the misorientation across the boundaries of the *mechanical* twins may deviate significantly from the ideal twin/matrix relationship due to the deformation-induced crystallographic rotations of the twin and matrix from their initial orientations. On the other hand, the misorientation across the boundaries of *annealing* twins would be expected to be close to the ideal 60° rotation about a <111> direction, because such twins do not undergo deformation. Thus, the deviation from the ideal $\Sigma 3$ misorientation may be used as a criterion to separate mechanical twins from annealing twins.

The distribution of the misorientation perturbation along the twin boundaries (within the Brandon interval) for the two times at room temperature is shown in Fig. 3c. After 2 weeks, the misorientation across the twin boundaries deviated significantly from the ideal relationship. This suggests that mechanical twins were most likely predominant in the microstructure. By contrast, after 11 months, perturbations from the ideal twin misorientation were much smaller, being within the typical accuracy of EBSD (2°). This latter observation indicates the formation of annealing twins prevailed during longer times.

Textures derived from low-resolution EBSD scans (for ~10,000-20,000 grains) are shown in terms of 111 pole figures in Fig. 4. For comparison purposes, the ideal textural components for simple-shear deformation (which characterizes HPT) of FCC metals [9] are also included in the figure. In all pole figures, the shear direction (SD) is horizontal, and shear plane normal (SPN) is vertical.

To a first approximation, the texture observed after 2 weeks at room temperature (Fig. 4a) can be described in terms of the superposition of partial 110 and 111 fibers; a tendency for the formation of the $B/\overline{B}$ simple-shear texture components was also noted (Fig. 4c). Part of the observed difference between the measured and ideal textures may be associated with a deviation between the experimental and theoretical shear direction/plane. Nevertheless, despite the large strain imposed during HPT, the texture was of only moderate strength, as is typical for shear textures in general.

After 11 months at room temperature, the texture was markedly different (Fig. 4b) in comparison to that seen after the shorter time. This trend was likely related to the observed grain growth. Although some texture peaks may be seen in the pole figure (Fig. 4b), their significance from a statistical standpoint was difficult to ascertain because of contamination by the orientations of the coarse, abnormal grains (Fig. 2c). In this regard, it was found that the abnormal grains themselves did *not* belong preferentially to any specific simple shear- or recrystallization texture component (e.g., cube or Goss), but rather had random crystallographic orientations. It is unlikely therefore that the observed abnormal grain growth was associated with the formation of a specific texture during or after cryogenic deformation.

In conclusion, severe cryogenic deformation of copper has been found to lead to very poor microstructure stability. Both normal and abnormal grain growth occur during long-time exposure at room temperature following such processing. Thus, the utility of cryogenic deformation for the production of nanocrystalline structures in copper appears to be limited.

The authors would like to acknowledge Professor G.A. Salishchev for suggesting this research. They also are grateful to Dr. R.M. Galeyev and Dr. O.R. Valiakhmetov for providing the material used in this work and to Professor H.J. Fecht, Dr. Julia Ivanisenko, and L. Kurmanaeva (Forshungszentrum Karlsruhe, Germany) for help in performing the cryogenic HPT experiments.

[1] Y. Huang, P.B. Prangnell, Acta Mater. 56 (2008) 1619.
[2] Y.S. Li, N.R. Tao, K. Lu, Acta Mater. 56 (2008) 230.
[3] Y. Zhang, N.R. Tao, K. Lu, Acta Mater. 56 (2008) 2429.
[4] H.D. Meingelberg, M. Meixner, K. Lucke, Acta Metal. 13 (1965) 835.
[5] I.A. Gindin, V.K. Aksenov, I.F. Borisova, Ya.D. Starodubov, Phys. Met. Metall. 39 (1975) 72.
[6] S.V. Dobatkin, G.A. Salischev, A.A. Kuznetsov, T.N. Kon'kova, Mater. Sci. Forum 558-559 (2007) 189.
[7] D. Dingley, J. Microscopy, 213 (2004) 214.
[8] F.J. Humphreys and M. Hatherly, Recrystallization and Related Annealing Phenomena, second ed., Elsevier, 2004.
[9] S. Li, I.J. Beyerlein, M.A.M. Bourke, Mater. Sci. Eng. A 394 (2005) 66.

Table 1. Nominal chemical composition (wt. %) of program material

O	Fe	Pb	S	Zn	Ag	Ni	As	Sb	Sn	Bi	Cu
0.05	0.005	0.005	0.004	0.004	0.003	0.002	0.002	0.002	0.002	0.001	Bal.

Figure Captions

Fig. 1. Effect of static storage at room temperature on Vickers microhardness. For comparison purposes, the microhardness of the as-received hot-rolled bar and "abc"-preconditioned material is also shown.

Fig. 2. Selected portions of EBSD maps of the microstructure after cryogenic high-pressure torsion and static storage at room temperature. LABs and HABs are depicted as red and black lines, respectively. RD, SD and SPN denote the radial direction, shear direction, and shear-plane normal, respectively,

Fig. 3. Effect of static storage time at room temperature on (a) the size distribution of the *fine* equiaxed grains, (b) misorientation-angle distribution and (c) misorientation perturbations along twin boundaries.

Fig. 4. Effect on texture of static storage at room temperature for (a) 2 weeks, or (b) 11 months. Figure (c) summarizes the ideal simple-shear texture components, as indicated by the various symbols (after Li, *et al.* [9]).

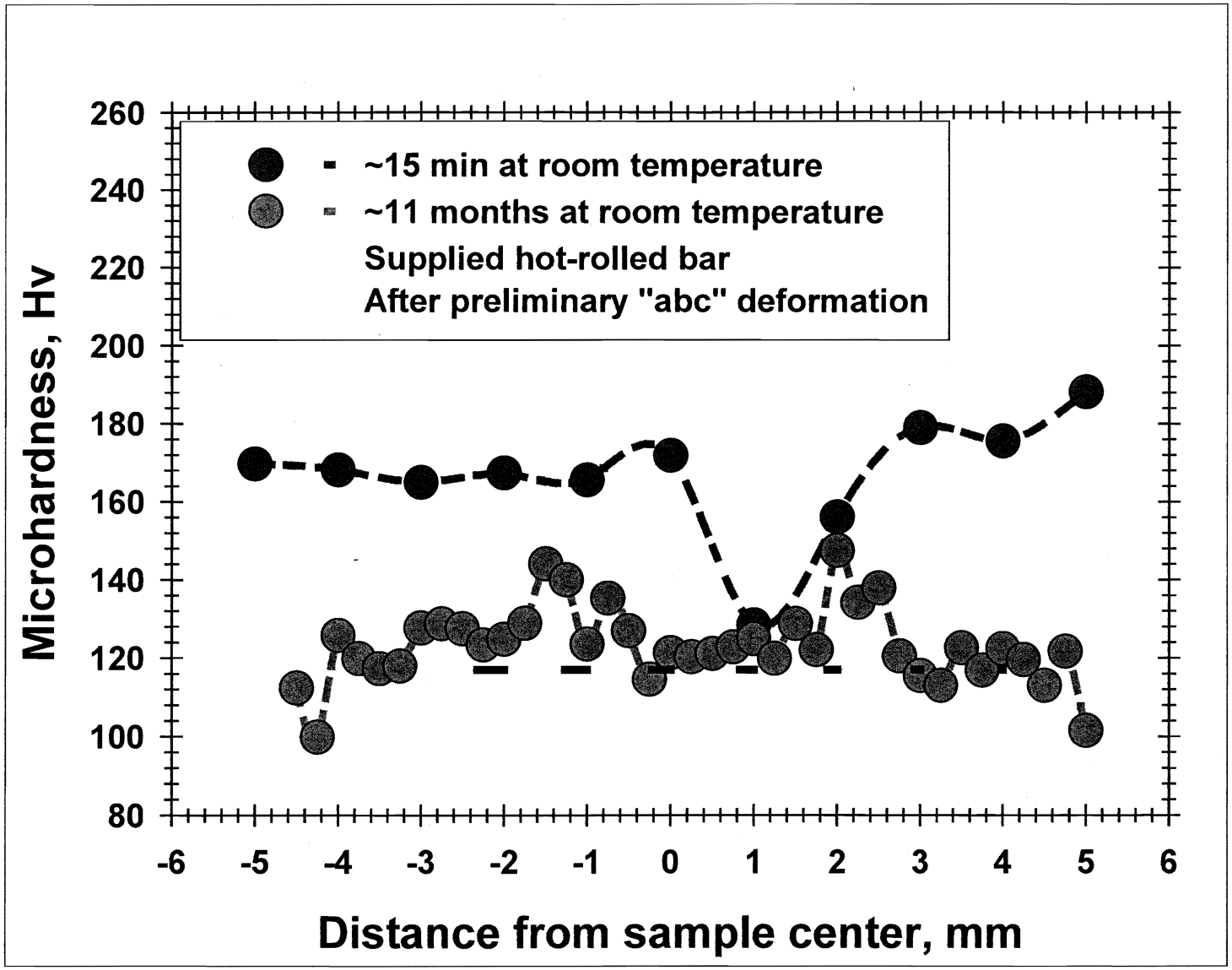

Fig. 1. Effect of static storage at room temperature on Vickers microhardness. For comparison purposes, the microhardness of the as-received hot-rolled bar and "abc"-preconditioned material is also shown.

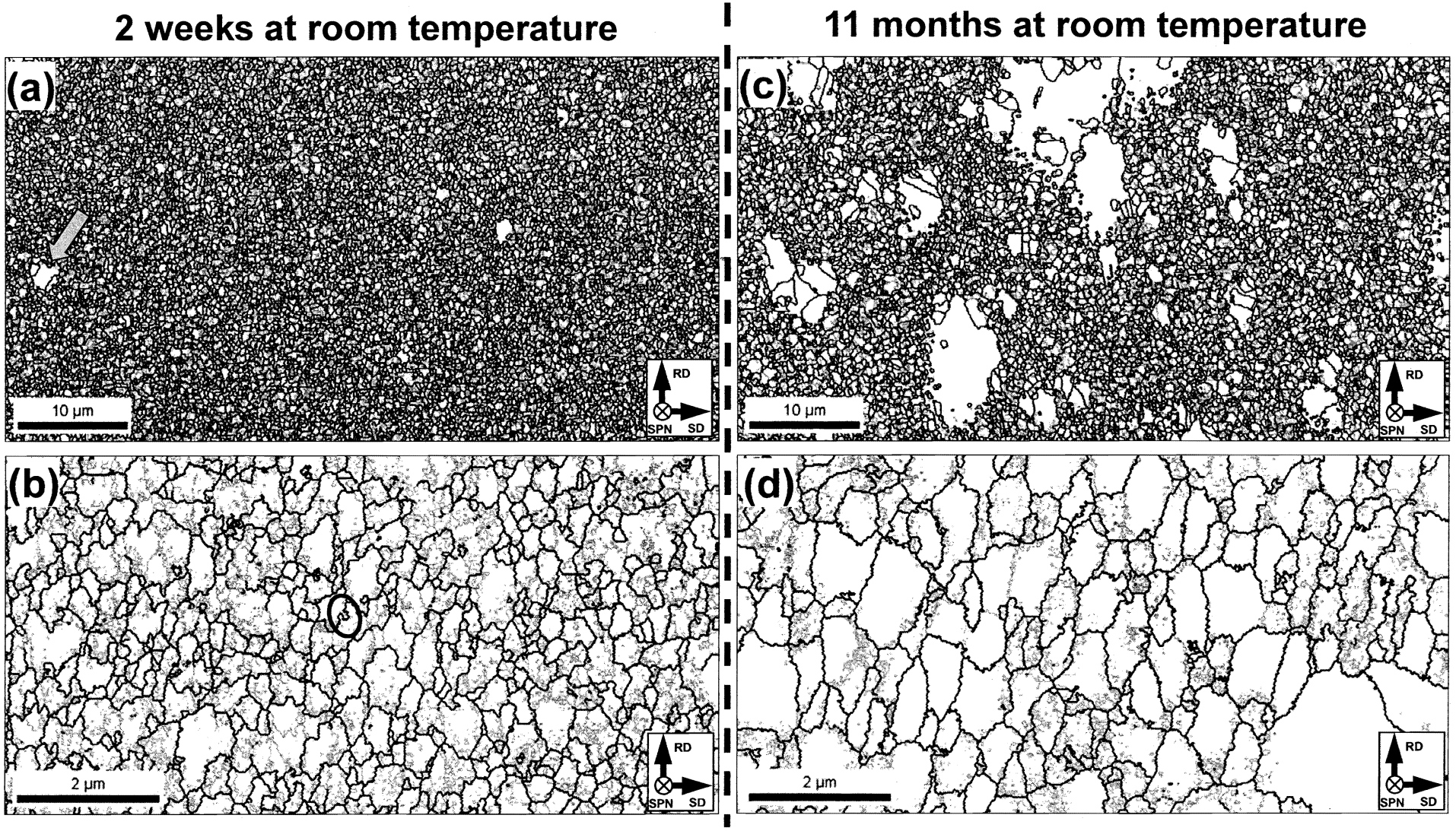

Fig. 2. Selected portions of EBSD maps of the microstructure after cryogenic high-pressure torsion and static storage at room temperature. LABs and HABs are depicted as red and black lines, respectively. RD, SD and SPN denote the radial direction, shear direction, and shear-plane normal, respectively,

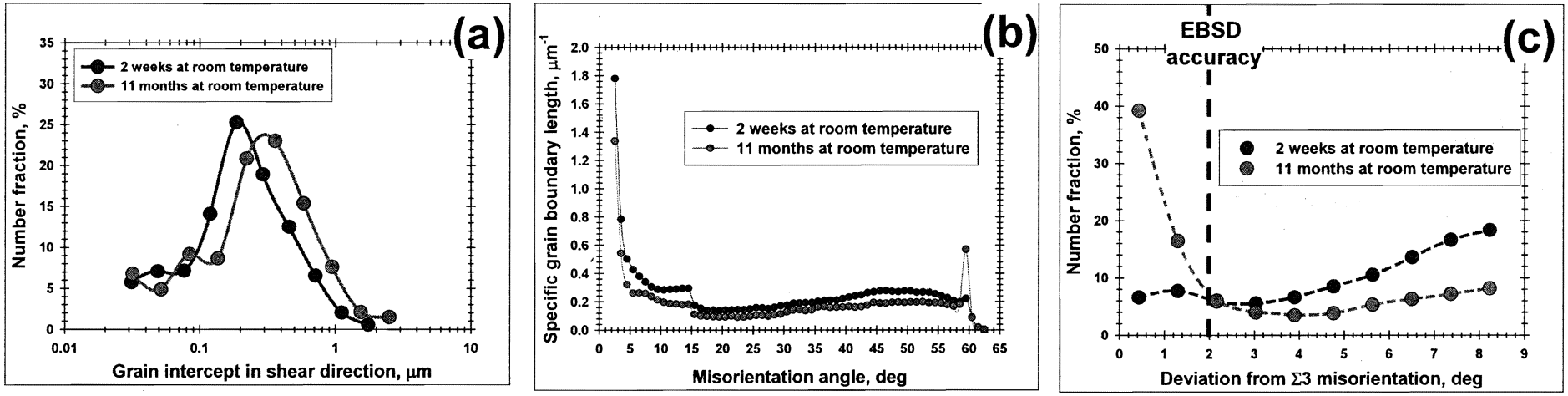

Fig. 3. Effect of static storage time at room temperature on (a) the size distribution of the *fine* equiaxed grains, (b) misorientation-angle distribution and (c) misorientation perturbations along twin boundaries.

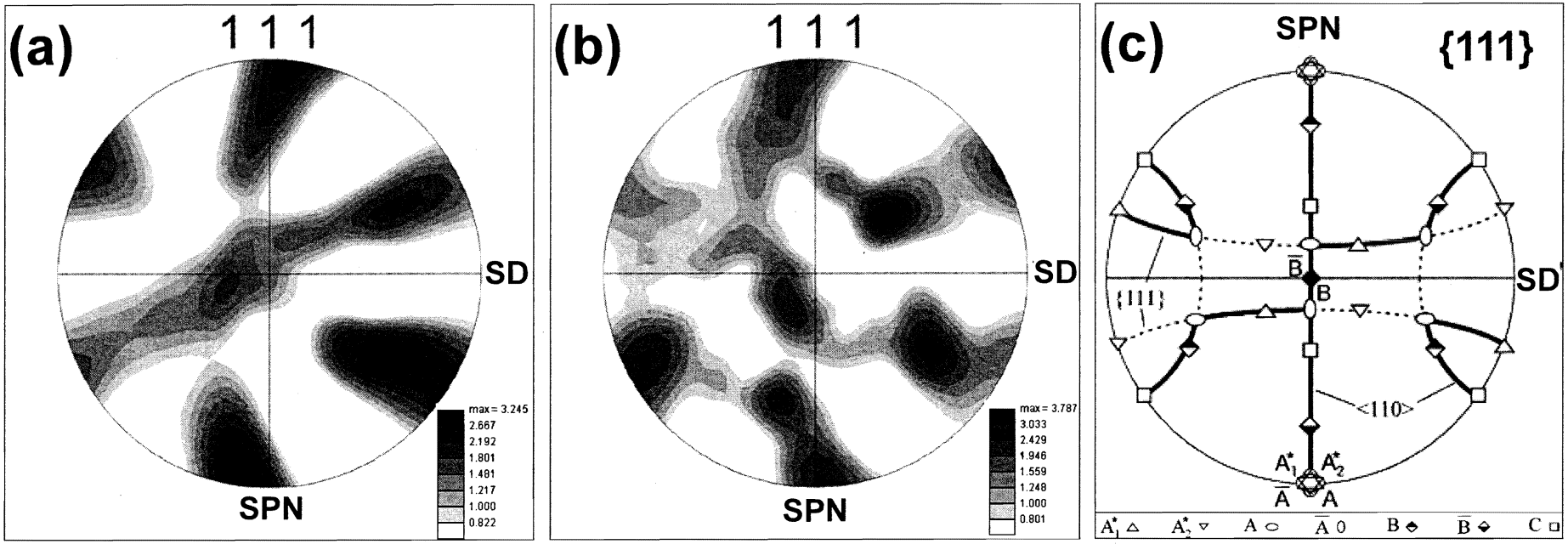

Fig. 4. Effect on texture of static storage at room temperature for (a) 2 weeks, or (b) 11 months. Figure (c) summarizes the ideal simple-shear texture components, as indicated by the various symbols (after Li, *et al.* [9]).